Supercritical Antisolvent Process for Substituted Para-Linked Aromatic Polyamides: Phase Equilibrium and Morphology Study

Sang-Do Yeo,[†] Pablo G. Debenedetti,*[,†] Maciej Radosz,*[,‡] and Hans-Werner Schmidt[§]

Department of Chemical Engineering, Princeton University, Princeton, New Jersey 08544, Corporate Research, Exxon Research and Engineering Company, Annandale, New Jersey 08801, and Materials Department, College of Engineering, University of California, Santa Barbara, California 93106

Received May 10, 1993; Revised Manuscript Received August 19, 1993[•]

ABSTRACT: Polycrystalline spherulites and microfibrils are obtained from a substituted para-linked aromatic polyamide in a supercritical antisolvent (SAS) process. Carbon dioxide is contacted with 0.03–0.12 wt % polymer in dimethyl sulfoxide and in *N,N*-dimethylformamide solutions in both batch and continuous modes of operation. Slow expansion of the solution produces polycrystalline spherulites in the 1–10-μm-diameter range, and the degree of crystallinity is affected by turbulence caused by carbon dioxide injection. A microfibrillar structure is obtained by spraying the polymer solution through a small orifice into cocurrently flowing supercritical carbon dioxide. This morphology is suggestive of shear-induced chain orientation during nucleation. In addition, phase boundaries of the polymer + solvent + antisolvent ternary and the solvent + antisolvent binary systems are determined up to 120 °C and 300 bar.

Introduction

Para-linked aromatic polyamides (aramids) are thermally stable polymers that can be used to produce high-modulus and heat-resistant fibers.[1] Because of the rigidity of the polymer backbone, they have unusual solution properties, including the formation of a lyotropic liquid crystalline phase in concentrated solutions. This liquid crystalline behavior is the key to process these materials toward high-modulus, high-tensile-strength fibers.[2] However, the limited solubility of unsubstituted rodlike aramids in common liquid solvents restricts the ease of processing, and hence the range of applications of such polymers. Recently, a variety of structural modifications of para-linked aromatic polyamides has been developed in order to increase the solubility, while at the same time maintaining the desirable properties of the parent polymers: extended-chain character, high glass transition temperature, and temperature stability.[3] This increased solubility not only may enhance existing processing routes, such as dry spinning, but also may open up new application areas, such as films, coatings, polymer blends, and composites. While liquid aprotic solvents are known to be effective in solubilizing the substituted aromatic polyamides, supercritical solvents or antisolvents have not been tried for polyamide processing.

However, the general concept of using a gas or a supercritical fluid as an antisolvent in polymer solutions is relatively well established.[4,5] For example, a supercritical antisolvent (SAS) has recently been used to produce a variety of polystyrene microparticles, including microspheres.[6] This approach has also been used to process proteins[7,8] and biodegradable polymers, such as poly(L-lactic acid).[9] The SAS process is especially attractive for biomedical applications because of its relatively mild operating conditions and the availability of a nontoxic antisolvent, such as carbon dioxide. The SAS process is based on the observation that the dissolution of a supercritical fluid in a liquid solvent is frequently accompanied by a large expansion of the liquid phase. This causes dissolved solutes to precipitate. Furthermore, in the vicinity of the solvent + SAS critical temperature, this expansion (dissolution of a supercritical fluid in a liquid solvent) depends sensitively on small changes in pressure. Also, above the dew point boundary, a single, antisolvent-rich phase can be formed. Thus, a major advantage of this process over those based on conventional liquid antisolvents is that, by a suitable choice of supercritical fluid and operating conditions, the solvent can be removed completely, extracted by the antisolvent, leaving behind a dry precipitate. Moreover, varying the rate at which the liquid and supercritical phases are brought into contact allows for controlling the rate of precipitation. This, in turn, affects the particle morphology, including the particle shape and size distribution.[8]

In this study, we select an example of a substituted para-linked aromatic polyamide that is relatively easy to dissolve in pure polar aprotic solvents. Our goals are, first, to understand the phase behavior of the aramid + solvent binary and aramid + solvent + antisolvent ternary systems and, second, to generate aramid particles by SAS precipitation, relating particle morphology to operating conditions.

Experimental Section

Materials. A substituted para-linked aromatic polyamide 8[3c] was synthesized by polycondensation of 2,2′-dimethyl-*N,N′*-bis(trimethylsilyl)-4,4′-diaminobiphenylene and biphenyl-2,5-dicarbonyl chloride. The inherent viscosity of 0.5% (w/v) polyamide 8 in *N,N*-dimethylacetamide/LiCl (4%, w/v) solution was 3.81 (dL/g).[3c] The molecular structure of polyamide 8 is as follows:

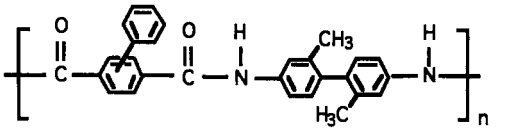

Dimethyl sulfoxide (DMSO; Fisher Scientific, Lot No. 911680) and *N,N*-dimethylformamide (DMF; Fisher Scientific, Lot No. 911251) were selected because of their high affinity to both polyamide 8 (solubility >5 wt %) and carbon dioxide (high

* To whom correspondence should be addressed.
† Princeton University.
‡ Exxon Research and Engineering Company.
§ University of California.
• Abstract published in *Advance ACS Abstracts*, October 15, 1993.

0024-9297/93/2226-6207$04.00/0

expansivity).[8] Liquid carbon dioxide of bone-dry grade (99.8%) was purchased from MG Industries. Solutions of polyamide 8 + DMSO and polyamide 8 + DMF are prepared in the concentration range of 0.03–0.12 wt % polymer.

Apparatus and Procedure. The phase boundaries of the polymer + DMSO + carbon dioxide solutions are measured in a batch optical cell (3.9 mL) equipped with a sapphire window, a movable piston, and a borescope camera. The SAS precipitation experiments and nucleation threshold measurements are conducted in a Jerguson gauge (Model 1940, view window, 75 mL). Two modes of operation, batch and continuous, are used for the SAS experiments. Detailed descriptions of the apparatus and operating procedures have been published elsewhere (see ref 8 for SAS experiments and ref 10 for phase boundary measurements), so only a brief overview is therefore given here.

The variable-volume optical batch cell is filled with 0.35 mL of the DMSO solution (either without or with 0.1 or 1.0% w/w polymer) and charged with liquid CO_2 up to 59.0 bar at 21.0 °C. The composition of the cell content is calculated using liquid CO_2 density data[11] and the known amount and composition of the DMSO + polymer solution. The polymer precipitation is observed through a video monitor connected to a borescope camera.

The cell temperature can be adjusted with an electric heater. The cell pressure can be adjusted with a movable piston, until the vapor and liquid phases merge into a single clear fluid phase in equilibrium with the solid phase. With stirring, temperature and pressure can equilibrate in 4 h and can be maintained within ±0.2 °C and ±0.5 bar, respectively.

While in the fluid + solid region, the pressure is decreased slowly (typically 0.2 bar/s, while stirring) until the clear fluid phase becomes cloudy. This onset of turbidity is used to locate the phase transition from fluid + solid to vapor + liquid + solid. The pressure is then increased by about 5 bar to obtain the clear fluid phase again, and this procedure is repeated several times. Deviations in the observed transition pressures are typically within ±0.5 bar.

In the batch mode of operation, the Jerguson gauge used for SAS experiments is initially loaded with 15 mL of polymer solution. As supercritical CO_2 is injected from the bottom of the Jerguson gauge, pressure is allowed to increase at two different rates: 20.6 or 0.8 bar/min, up to 103.4 bar. The increasing pressure enhances the solubility of CO_2 in the solution, which causes the solution to expand and, eventually, the polymer to precipitate. The particles are dried by flowing supercritical CO_2 at 103.4 bar and 35 °C through the Jerguson gauge for 2 h at a rate of 8.0 standard L/min (SLPM). During the slow injection of CO_2, the threshold pressure at which the DMSO solution becomes suddenly cloudy is recorded. This event is taken to be the onset of polymer nucleation in the bulk solution and to coincide with a phase transition boundary from vapor + liquid to vapor + liquid + solid, because of its sharpness and reproducibility. This threshold nucleation pressure (cloud point) is measured as a function of temperature.

In the continuous mode of operation, CO_2 flows downward through the Jerguson gauge at 103.4 bar and 8.0 SLPM. The polymer solution is pumped cocurrently into the Jerguson gauge through a nozzle (Ted Pella; 30-μm diameter, 0.24-mm thickness, platinum) at 120 bar and 0.3 mL/min. The nucleation is observed as a cloud formation about 1 cm apart from the nozzle exit, where the small droplets of the solution expand and dissolve ("evaporate") into the CO_2 phase. This mode of operation allows a very rapid contact of the two phases, as well as rapid subsequent expansion and complete evaporation of the solvent. This is the major difference compared to the batch operation where the rate of expansion of the polymer solution (that is, the rate at which the solvent and SAS phases are contacted) is low.

The morphology of the precipitated polymer is examined by scanning electron microscopy (SEM; Model JEOL JSM 840A). The specimens are sputter-coated with gold–palladium.

Results and Discussion

A pressure–temperature phase diagram of the CO_2 + DMSO + polyamide 8 system is shown in Figure 1. The phase boundary points for the CO_2 + DMSO (12.2% w/w DMSO) binary system are shown as filled circles. This phase boundary is measured at constant composition. The CO_2 + DMSO + polymer ternary system is in the two-phase region (VL in Figure 1) at atmospheric pressure over the range of polymer compositions studied here. As the pressure is increased at constant temperature, polymer precipitation occurs, and the system enters the three-phase region (VLS in Figure 1). As pressure is increased further,

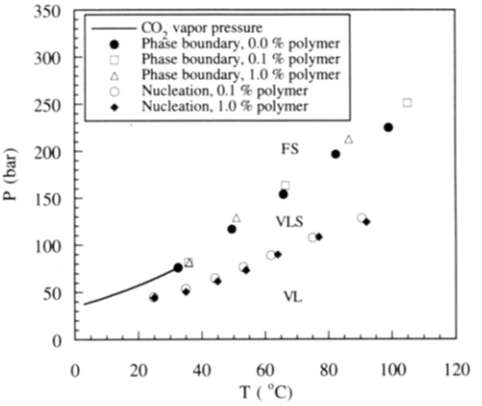

Figure 1. Equilibrium phase boundaries for the CO_2 + DMSO + polyamide 8 system, for 12.2% (w/w) DMSO, on a polymer-free basis. Polymer concentrations in DMSO solutions: 0.0, 0.1, and 1.0% (w/w). VL: vapor + liquid. VLS: vapor + liquid + solid. FS: fluid + solid.

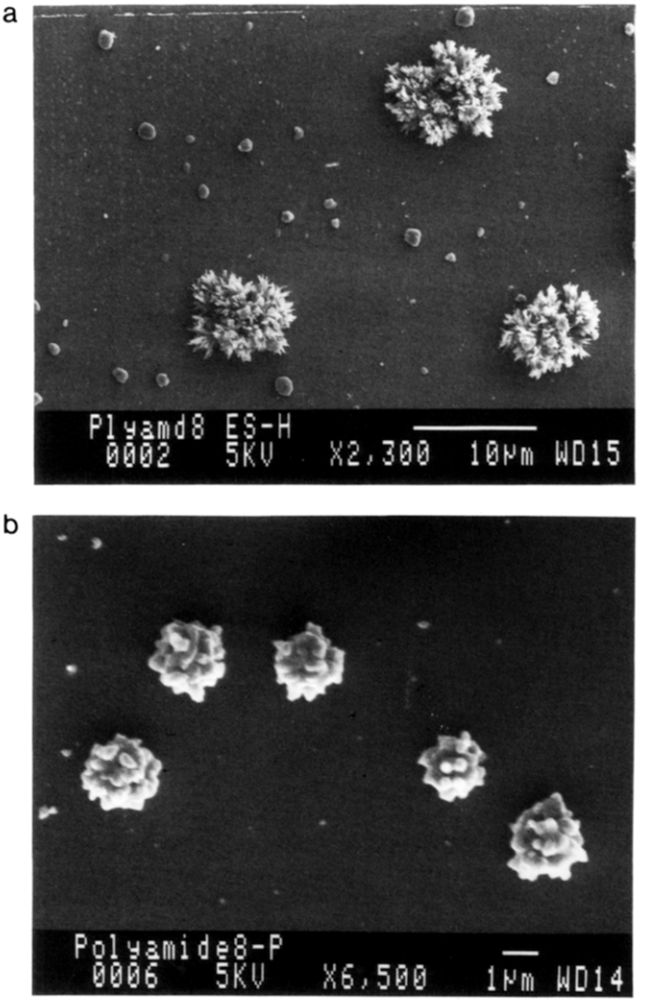

Figure 2. Polyamide 8 particles produced in a batch experiment. (a) DMSO, 0.12% (w/w), 23 °C, injection rate 0.8 bar/min, from 1 to 103.4 bar. (b) DMSO, 0.03% (w/w), 23 °C, injection rate 20.6 bar/min, from 1 to 103.4 bar.

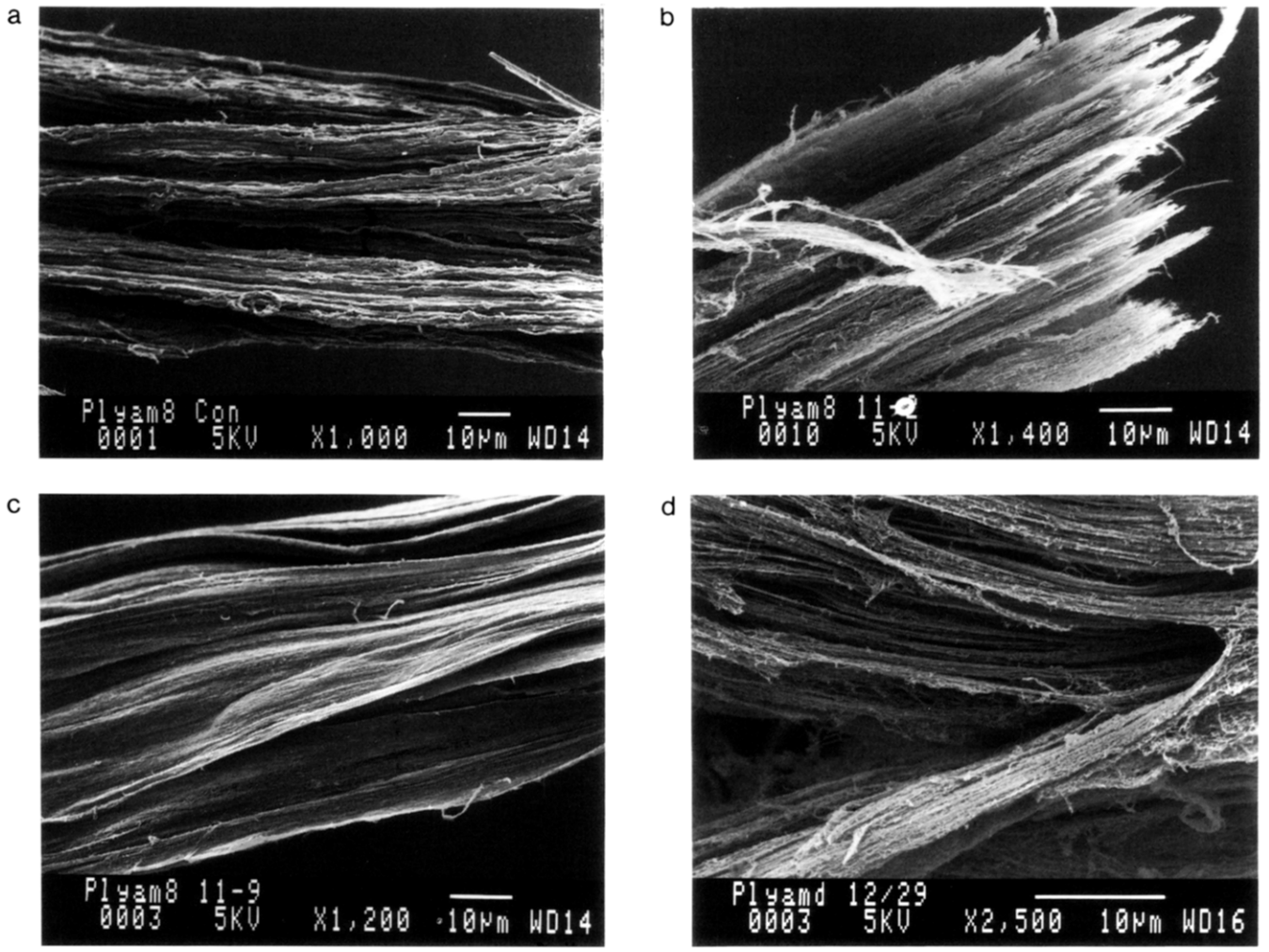

Figure 3. Polyamide 8 fibers produced in a continuous flow experiment at 103.4 bar. (a) DMSO, 0.03% (w/w), 23 °C (b) DMSO, 0.03% (w/w), 40 °C. (c) DMF, 0.03% (w/w), 23 °C. (d) DMSO, 0.09% (w/w), 40 °C.

the boundary between CO_2-rich (V) and DMSO-rich (L) phases disappears (V and L merge) in the presence of solid polymer, and the system enters the two-phase region labeled FS (fluid + solid) in Figure 1. The FS–VLS phase boundary at 32.5 °C is of the bubble-point type, whereas at 49.5 °C and above it is of the dew-point type. The FS–VLS boundary is quite insensitive to changes in the polymer concentration, as seen in Figure 1. The CO_2 + DMSO binary system shows type I phase behavior.[12] For this class of systems, the bubble-point curve is quite insensitive to composition in the low concentration range of the heavier compound.

The threshold nucleation pressure (cloud point) is not affected much by the initial polymer concentration in solution. A phase diagram such as that shown in Figure 1 allows the selection of desirable operating conditions for a SAS process. In general, operation in the FS region leads to polymer precipitation and removal of the solvent. On the other hand, in the VLS region, solvent removal is incomplete; in the VL region, the polymer does not precipitate.

Figure 2 shows SEM photomicrographs of polyamide 8 processed in a batch mode of operation. The slow expansion of the polymer solution, induced by the slow injection of CO_2 (0.8 bar/min, which maintains the system virtually undisturbed during the expansion), provides a stable environment for the formation of a spherulitic network of lamellar crystals. Two steps are thought to be involved:[13] (1) One is the formation of individual lamellae from a single crystal nucleus. Since rodlike para-linked polyaramids show no evidence of chain folding due to the chain rigidity,[14] the orientation of the polymer chains inside the lamellae is expected to be parallel to the lamellar axis, in contrast to that of a folded chain. (2) The other is extension and growth of the lamellar crystals outward from the nucleus (Figure 2a), accompanied by interlamellar junctions, as well as interlamellar organization that tends to produce a spherical envelope of ca. 10 μm in diameter.[15,16] A nonspherulitic structure (Figure 2b) is obtained with a higher injection rate (20.6 bar/min), which causes visible turbulence during nucleation. This turbulence disrupts the oriented packing of the polymer chains and hence results in spheroidal primary particles which undergo coalescence toward star-shaped particles. The spheroidal morphology of the primary particle can be due to the low-crystalline or amorphous nature of the polymer particles. The crystallization mechanism in the batch experiment is analogous to that which occurs during precipitation caused by controlled evaporation of a liquid solvent. In this static process, with or without turbulence, there is no external force involved during the precipitation stage.

However, in the continuous mode of operation, the polymer solution is sprayed into the cocurrently flowing CO_2 phase and it undergoes a shear stress caused by the different flow rates of the two phases. Visible nucleation occurs in the presence of the shear before the two phases completely coalesce into a single stream. Hence, in the precipitation stage, the randomly-oriented polymer chains undergo an alignment (due to drawing) in the direction of the applied stress. This effect, combined with the rapid

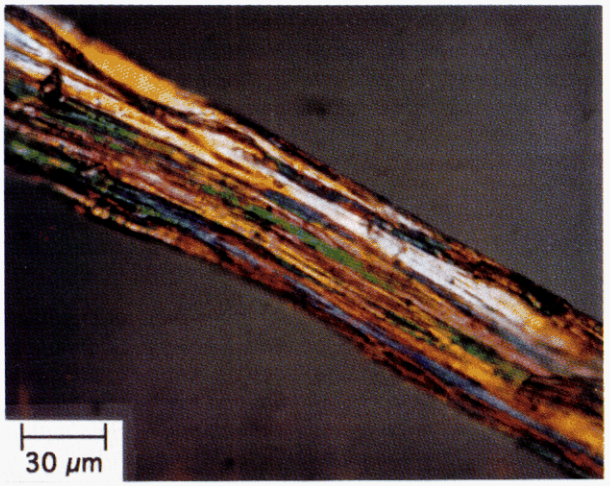

Figure 4. Polyamide 8 fiber shown in Figure 3a, observed under an optical microscope equipped with a cross polarizer.

expansion of the solution, leads to a fibrous morphology shown in Figure 3. The direction of the polymer chains in these fibers must be parallel to the fiber axis. The stiffness of the aramid backbone and the ability of forming intermolecular hydrogen bonds[17] also contribute to the ease of fiber formation. In contrast, semicrystalline, flexible-chain polymers, such as poly(L-lactic acid),[9] and noncrystalline polymers, such as polystyrene,[6] produced spherical amorphous particles under similar SAS operating conditions. The fibrous structure (Figure 3) is obtained with both solvents (DMSO and DMF), as well as over the whole concentration and temperature ranges investigated, which suggests a consistent, robust process.

The SEM photomicrographs shown in Figure 3 suggest that the fiber consists of a stack of microfibrils of 0.1–1 μm in diameter and that the smaller fibrils are not resolved. The material processed at higher temperature (40 °C) is found to contain finer fibrils. Figure 4 shows one such fiber observed under an optical microscope with a cross polarizer. Different colors observed along the fiber suggest a high degree of orientation within each fibril. This may be due to the fact that, upon expansion, the polymer-containing solution crosses the critical concentration of the polymer with respect to formation of liquid crystalline phases. If this is the case, the precipitation occurs from the liquid crystalline state. During the nucleation of a liquid crystalline solution, the orientation of crystalline domains should be affected by the rate of nucleation and the presence of external forces. In general, depending on whether the solution is quiescent or agitated or whether a shear stress is applied, precipitation gives rise to polycrystalline spherulites, low-crystallinity particles, and oriented (chain-extended) fibers.

Conclusions

The phase diagram, measured for aromatic polyamide + solvent binary and polyamide + solvent + CO_2 ternary systems, is used to rationalize and explain the morphology of polymer particles formed in SAS processing. Polyamide microspherulites of a varying degree of crystallinity, from amorphous to semicrystalline, and microfibrils are demonstrated in batch and continuous SAS experiments. The SAS-formed fibers are found to contain oriented aramid molecules.

Acknowledgment. P.G.D. gratefully acknowledges the National Science Foundation (Grant CTS-9000614) for partial support of this work. M.R. gratefully acknowledges unpublished data on supercritical antisolvent experiments on CO_2 + toluene + polystyrene provided by Keith P. Johnston (University of Texas, Austin).

References and Notes

(1) Cassidy, P. E. *Thermally Stable Polymers*; Marcel Dekker: New York, 1980.
(2) (a) Kwolek, S. L.; Morgan, P. W.; Schaefgen, J. R. In *Encyclopedia of Polymer Science and Engineering*; Mark, H. F., Bikales, N. M., Overberger, C. G., Menges, G., Eds.; Wiley: New York, 1987; Vol. 9, p 1. (b) Yang, H. H. *Aromatic High Strength Fibers*; Wiley: New York, 1989.
(3) (a) Jadhav, J. Y.; Preston, J.; Krigbaum, W. R. *J. Polym. Sci., Part A: Polym. Chem.* **1989**, *27*, 1175. (b) Gaudiana, R. A.; Minns, R. A.; Sinta, R.; Weeks, N.; Rogers, H. G. *Prog. Polym. Sci.* **1989**, *14*, 47. (c) Hatke, W.; Schmidt, H.-W.; Heitz, W. *J. Polym. Sci., Part A: Polym. Chem.* **1991**, *29*, 1387.
(4) McHugh, M. A.; Guckes, T. L. *Macromolecules* **1985**, *18*, 674.
(5) Seckner, A. J.; McClellan, A. K.; McHugh, M. A. *AIChE J.* **1988**, *34*, 9.
(6) Dixon, D. J.; Johnston, K. P.; Bodmeier, R. A. *AIChE J.* **1993**, *39*, 127.
(7) Tom, J.; Lim, G.; Debenedetti, P. G.; Prud'homme, R. K. In *Supercritical Fluid Engineering Science*; Kiran, E., Brennecke, J. F., Eds.; ACS Symposium Series 514; American Chemical Society: Washington, DC, 1993; Chapter 19.
(8) Yeo, S.; Lim, G.; Debenedetti, P. G.; Bernstein, H. *Biotechnol. Bioeng.* **1993**, *41*, 341.
(9) Randolph, T. W.; Randolph, A. D.; Mebes, M.; Yeung, S., submitted for publication in *Biotechnol. Prog.*
(10) (a) Chen, S.; Radosz, M. *Macromolecules* **1992**, *25*, 3089. (b) Gregg, C. J.; Stein, F. P.; Morgan, C. K.; Radosz, M., submitted for publication in *J. Chem. Eng. Data.*
(11) Angus, S.; Armstrong, B.; deReuck, K. M. *IUPAC, International Thermodynamic Tables of the Fluid State: Carbon Dioxide*; Pergamon Press: Elmsford, NY, 1976.
(12) Rowlinson, J. S.; Swinton, F. L. *Liquids and Liquid Mixtures*, 3rd ed.; Butterworths Scientific: London, 1982; p 203.
(13) Odian, G. *Principles of Polymerization*, 3rd ed.; John Wiley & Sons: New York, 1991; p 26.
(14) Mark, H. F.; Bikales, N. M.; Overberger, C. G.; Menges, G. *Encyclopedia of Polymer Science and Engineering*; John Wiley & Sons: New York, 1988; Vol. 11, p 383.
(15) Bush, P. J.; Pradhan, D.; Ehrlich, P. *Macromolecules* **1991**, *24*, 1439.
(16) Bassett, D. C. *Principles of Polymer Morphology*; Cambridge University Press: London, 1981; p 19.
(17) Northolt, M. G. *Eur. Polym. J.* **1974**, *10*, 799.